Structure of $Ba_3In_2O_5F_2$ by Combined Powder X-Ray and Neutron Diffraction Analysis; Oxide/Fluoride Ordering in a Ruddlesden–Popper Phase

Richard L. Needs and Mark T. Weller
Department of Chemistry, University of Southampton, Southampton SO17 1BJ, UK

The structure of a new fluoride oxide $Ba_3In_2O_5F_2$ has been determined from the simultaneous refinement of powder X-ray and powder neutron diffraction data. This Ruddlesden–Popper type phase crystallises in the space group *I4/mmm* with lattice parameters $a = 4.18$ and $c = 22.82$ Å. The structure shows ordering of the oxide and fluoride ions, as evidenced from bond valence considerations, producing sheets of vertex-sharing indium–oxygen square pyramids separated by BaF layers.

In the structural chemistry of complex fluoride oxides only a few examples of materials with ordered oxide and fluoride ions are well characterised. The sizes of these two anions are similar and the anions frequently adopt a random distribution over the various sites available, *e.g.* FeOF, NbO_2F, $KCrO_3F$ and the Aurivillius-type phases such as Bi_2NbO_5F and $Bi_2TiO_4F_2$.[1-4] A few materials are known to have ordered fluoride and oxide ions such as ScOF and rhombohedral fluorite-type lanthanide fluoride oxides, *e.g.* $ThOF_2$ and pyrochlore structure fluoride oxides such as $CdNdTi_2O_6F$.[5-8] We have recently reported the synthesis and structure of Ba_2InO_3F[9] in which ordering of oxide and fluoride anions over the apical and in-plane sites is clear from the adoption of a low-symmetry variation of the K_2NiF_4 structure; ordering is also apparent from consideration of the bond-valence sums in this structure. More recent work has shown that Ba_2InO_3F is a member of a large family of fluoride oxides containing trivalent cations with structures based on K_2NiF_4 and the Ruddlesden–Popper phases. A number of these materials display ordered oxide and fluoride ions as evidenced by the symmetry and bond-valence parameters.

Two Ruddlesden–Popper halide oxides of indium, $Ba_3In_2O_5Cl_2$[10] and $Ba_3In_2O_5Br_2$,[11] have been reported by Müller-Buschbaum and co-workers; with the larger halides, ordering of the anions is expected and clearly seen in the structures. In this article we report the structure of $Ba_3In_2O_5F_2$ as determined from a combined refinement of powder X-ray and powder neutron diffraction data. This determines the structure of the polycrystalline material as accurately as possible and produces the most reliable positional parameters. A combined refinement utilises the ability of neutron diffraction to delimit light-atom positions precisely in the presence of barium and with time-of-flight data provides reliable thermal parameters, whilst X-ray diffraction locates the heavy barium accurately and minimises the adverse effects of the substantial indium neutron absorption on the thermal parameters. Hence, bond lengths are defined accurately, which is essential for fluoride and oxide site assignments using bond-valence methods.

Experimental

The compound $Ba_3In_2O_5F_2$ was prepared by the direct solid-state reaction of an intimate mixture of $BaCO_3$, In_2O_3 and BaF_2 in the correct stoichiometric proportions at 1050 °C. Powder X-ray diffraction data were collected from the pale grey-green product and showed the sample to be monophasic and crystalline. The pattern was indexed as a tetragonal unit cell with $a = 4.18$ and $c = 22.82$ Å, typical for a phase crystallising with the $Sr_3Ti_2O_7$ structure type.

Structure Determination

Powder X-ray diffraction data were collected using a Siemens D5000 diffractometer employing Cu-Kα_1 radiation ($\lambda = 1.5406$ Å) over the range 2θ 20–120°. Powder neutron diffraction data were collected on the POLARIS medium-resolution diffractometer at the Rutherford-Appleton Laboratory over the time-of-flight range 3–19 ms. Data from the high-resolution back-scattering bank were used for the refinement. The data were analysed using the GSAS package[12] running on an HP735 workstation and the combined X-ray and neutron diffraction data sets were refined simultaneously from a single coordinate set. Neutron-scattering lengths and absorption cross-sections were taken from Koster and Yelon.[13]

The initial structural model was based on that of $Sr_3Ti_2O_7$ in the space group *I4/mmm* with indium on 4e $(0,0,z)$, $z \approx 0.1$, anions X (1) on 4e $(0,0,z)$, $z \approx 0.20$, X (2) on 8g $(\frac{1}{2},0,z)$, $z \approx 0.1$ and X (3) on 2a (0,0,0) and barium ions on 2b $(0,0,\frac{1}{2})$ and 4e $(0,0,z)$, $z \approx 0.33$. In the initial stages no attempt was made to distinguish the anion sites and all positions were given scattering powers appropriate to oxygen; in the later stages of the refinement attempts were made to distinguish fluorine and oxygen on the anion sites but no significant change in the fit parameters was obtained by doing so. Assignment of specific sites to fluorine and oxygen was therefore carried out by way of bond-valence considerations, see below. The refinement proceeded smoothly with the latter stages of refinement allowing the introduction of anisotropic thermal parameters on all atoms. Upon close inspection of the neutron-profile fit a small but significant level of impurity was observed. The majority of the impurity was successfully accounted for by the inclusion of Ba_2InO_3F as a second phase using the atomic coordinates from a single-phase time-of-flight refinement.[14] Final atomic positions and thermal parameters are given in Table 1 and derived bond lengths summarised in Table 2. Final fit factors were neutron $R_{wp} = 0.0177$, X-ray $R_{wp} = 0.1261$, overall $x^2 = 7.33$. The final profile fits to the data are shown in Fig. 1(*a*), 1(*b*) and 2.

Discussion

Considerations of the co-ordination geometries of the three anion sites may be used to assign fluoride and oxide ions. Bond-valence calculations were carried out for each anion site. The

Table 1 Final refined atomic coordinates for $Ba_3In_2O_5F_2$ at 298 K with estimated standard deviations (e.s.d.s.) in parentheses

					Anisotropic thermal parameter/Å^2		
Atom	Site	*x*	*y*	*z*	B_{11}	B_{22}	B_{33}
Ba(1)	4e	0.0	0.0	0.323 19(7)	1.33(5)	1.33(5)	1.02(8)
Ba(2)	2b	0.0	0.0	$\frac{1}{2}$	1.24(7)	1.24(7)	2.0(20)
In	4e	0.0	0.0	0.090 83(8)	0.69(4)	0.69(4)	0.82(10)
O(1)	8g	0.0	$\frac{1}{2}$	0.103 12(7)	1.53(6)	0.53(5)	3.16(10)
O(2)	2a	0.0	0.0	0.0	3.64(12)	3.64(12)	0.13(12)
F	4e	0.0	0.0	0.204 6(1)	3.79(9)	3.79(9)	1.68(11)

Space group *I*4/*mmm*; *a* = 4.1844(1), *c* = 22.8229(6) Å.

Table 2 Calculated interatomic distances (Å) and selected angles (°) with e.s.d.s in parentheses

In–O(1)	4 × 2.1109(3)	Ba(1)–F	1 × 2.705(4)
In–O(2)	1 × 2.073(2)	Ba(1)–O(1)	4 × 2.684(1)
In–F	1 × 2.598(4)	Ba(2)–O(1)	8 × 3.149(1)
Ba(1)–F	4 × 3.0262(7)	Ba(2)–O(2)	4 × 2.9588(1)
O(1)–In–O(1)	164.7(1)	O(1)–In–O(2)	97.64(6)

Table 3 Bond valence calculations. Values are per bond; summations allow for bond multiplicity

	O(1)	O(2)	F	Sum
Ba(1)	0.097	—	0.104 0.247	2.02
Ba(2)	0.340	0.160	—	1.80
In	0.569	0.630	0.113	3.02
Sum	2.01	1.91	0.77	

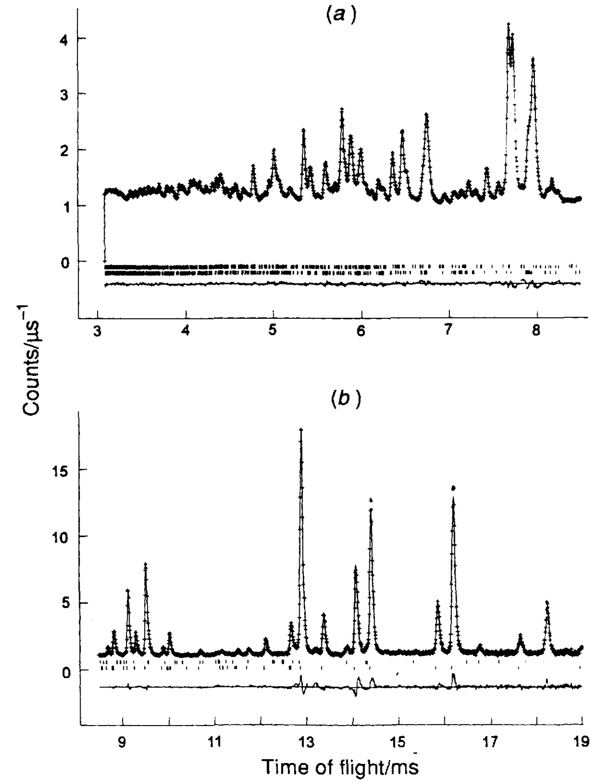

Fig. 1 Profile fit to the powder neutron diffraction data. Crosses are the observed points, the upper continuous line is the calculated profile, and the lower continuous line the difference. Tick marks show the reflection positions (upper set Ba_2InO_3F, lower set $Ba_3In_2O_5F_2$)

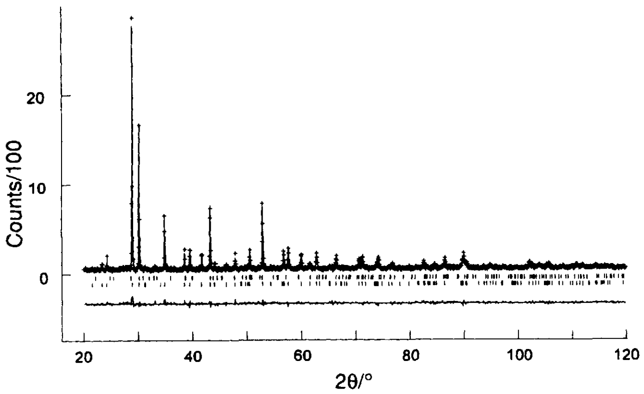

Fig. 2 Profile fit to the powder X-ray diffraction data. Crosses are the observed points, the upper continuous line is the calculated profile, and the lower continuous line the difference. Tick marks show the reflection positions (upper set Ba_2InO_3F, lower set $Ba_3In_2O_5F_2$)

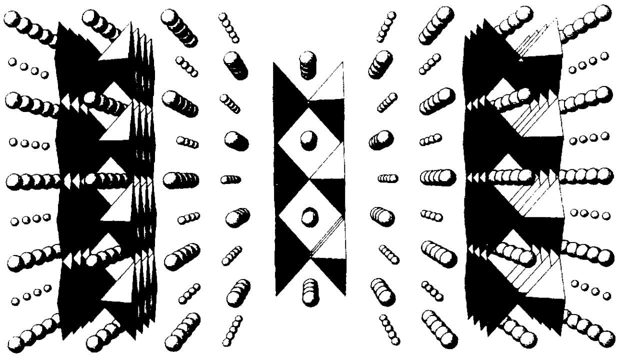

Fig. 3 Structure of $Ba_3In_2O_5F_2$. The InO_5 square pyramids are shown as shaded polyhedra separated by double BaF layers

bond valency[14] obtained for oxide on the 4e site (ideally 2.0) is unacceptably low at 1.01, whilst values of 2.01 and 1.91 were obtained for the other two sites. Placement of a fluoride ion on 4e gives a reasonable value for the fluoride bond valence of 0.77 (ideally 1.0), whilst fluoride on the 2a or 8g sites gives unacceptably high values. These values and those for the cations are summarised in Table 3.

The refined geometry around the indium site is similar to that found in Ba_2InO_3F with square-pyramidal geometry with respect to oxide plus one much longer interaction to fluoride. The structure can, therefore, be considered to consist of double layers of vertex-sharing InO_5 square pyramids separated by BaF layers (Fig. 3).

The structure of $Ba_3In_2O_5F_2$ can be compared to those of $Ba_3In_2O_5Cl_2$ and $Ba_3In_2O_5Br_2$. The *c* lattice parameter increases markedly from X = F (22.8229) through X = Cl (24.929) to X = Br (25.8552 Å) reflecting the increasing capping

Ba–X distance in the capped anti-square-prismatic co-ordination. The *a* lattice parameter also increases marginally from X = F (4.1884) through Cl (4.2359) to Br (4.2546 Å). The geometry around the indium site is approximately square pyramidal in each case with a short apical In–O bond, though with the fluoride ion this is slightly longer (2.07 Å) than with chloride and bromide (2.05 Å) probably indicating a residual *trans* In–X interaction which exists only for X = F.

In conclusion, whilst many fluoride oxide structures reported in the literature thus far show randomly distributed anions, it is clear from $Ba_3In_2O_5F_2$ and Ba_2InO_3F that where the possibility exists for segregation of fluoride ions such ordering behaviour can occur, completely segregating the two different anions. However, in some materials such as K_2NbO_3F,[15] whilst the fluoride ions probably occupy the apical sites these two positions are randomly occupied by equal amounts of oxide and fluoride and the cell symmetry is tetragonal. We have investigated the structures of a number of fluoride oxides containing trivalent cations with K_2NiF_4 and $Sr_3Ti_2O_7$ type arrangements and found fluoride-ion ordering in the majority. However, in some, *e.g.* Ba_2ScO_3F the apical sites are randomly occupied by fluoride and oxide. The structures of these materials will be reported elsewhere.

Acknowledgements

We thank the EPSRC for a grant in support of this work and the University of Southampton for a partial studentship support for R. L. N.

References

1 M. Vlasse, J.-C. Massies and G. Demazeau, *J. Solid State Chem.*, 1973, **8**, 109.
2 F. P. Gortsema and R. Didchenko, *Inorg. Chem.*, 1980, **4**, 182.
3 J. A. A. Ketelaar and E. Wegerif, *Recl. Trav. Chim. Pays-Bas*, 1938, **57**, 1269.
4 I. H. Ismailzade and J. Ravez, *Ferroelectrics*, 1978, **21**, 423.
5 M. Vlasse, M. Saux, P. Echegut and G. Villeneuve, *Mater. Res. Bull.*, 1979, **14**, 807.
6 J. Lucas and J.-P. Rannou, *C.R. Hebd. Seances Acad. Sci., Ser. C*, 1968, **266**, 1056.
7 J.-P. Rannou and J. Lucas, *Mater. Res. Bull.*, 1969, **4**, 443.
8 J. Grannec, H. Baudry, J. Ravez and J. Portier, *J. Solid State Chem.*, 1974, **10**, 66.
9 R. L. Needs and M. T. Weller, *J. Chem. Soc., Chem. Commun.*, 1995, 353.
10 W. Gutau and H. K. Müller-Buschbaum, *Z. Anorg. Allg. Chem.*, 1990, **584**, 125.
11 M. Abed and H. K. Müller-Buschbaum, *J. Alloys Compd.*, 1992, **183**, 24.
12 A. C. Larson and R. B. Von Dreele, GSAS Generalized Structure Analysis System, MS-H805, Los Alamos, NM, 1990.
13 L. Koster and W. B. Yelon, *Neutron Diffraction Newsletter*, 1982.
14 R. L. Needs and M. T. Weller, unpublished work.
15 F. Galasso and W. Darby, *J. Phys. Chem.*, 1962, **66**, 1318.

Received 15*th March* 1995; *Paper* 5/01646K